Liquid Crystals
Publication details, including instructions for authors and subscription information:
http://www.informaworld.com/smpp/title~content=t713926090

Preparation and evaluation of novel ferroelectric liquid crystalline cyclic siloxane tetramers

D. Lacey[a]; E. T. Mann[b]
[a] Department of Chemistry, Faculty of Science University of Hull Hull HU6 7RX UK, [b] PETA Solutions, Perkin Elmer Chalfont Road, Seer Green Beaconsfield, HP9 2FX UK,

Online publication date: 11 November 2010

To cite this Article Lacey, D. and Mann, E. T.(2003) 'Preparation and evaluation of novel ferroelectric liquid crystalline cyclic siloxane tetramers', Liquid Crystals, 30: 10, 1159 — 1170
To link to this Article: DOI: 10.1080/02678290310001599224
URL: http://dx.doi.org/10.1080/02678290310001599224

LIQUID CRYSTALS, VOL. 30, NO. 10, OCTOBER, 2003, 1159–1170

Preparation and evaluation of novel ferroelectric liquid crystalline cyclic siloxane tetramers

D. LACEY*
Department of Chemistry, Faculty of Science, University of Hull, Hull HU6 7RX, UK

and T. E. MANN
PETA Solutions, Perkin Elmer, Chalfont Road, Seer Green, Beaconsfield, HP9 2FX, UK

(*Received 31 March 2003; accepted 14 May 2003*)

Two series of liquid crystalline cyclic siloxane tetramers, one containing the 2-methylbutyl chiral group and the other the 1-methylheptyl chiral group, were prepared to investigate, in a systematic manner, the role of molecular structure of (a) the spacer group, (b) the mesogenic side chain and (c) the chiral end group, on the liquid crystalline behaviour of these novel tetramers. The results from this systematic structure/property correlation study clearly showed the effect of the structure of both the chiral end group and the mesogenic side chain core on the thermal properties and temperature ranges of the SmC* phase (ferroelectric) exhibited by these novel materials. By the appropriate choice of spacer group, mesogenic side chain and chiral end group, a number of cyclic siloxane tetramers exhibiting wide SmC* ranges (ferroelectricity) around room temperature were synthesized.

1. Introduction

Although a substantial number of polymer backbones have been used to synthesize side chain liquid crystalline (SCLC) polymers for a variety of applications, there has still been little research work carried out in the interesting area of cyclic SCLC oligomers [1–4], even though these polymers have been shown to be useful materials for optical data storage devices [5], optical filters [6] and reversible holographic-optical data storage devices [7]. It has been suggested [8, 9] through molecular modelling that because of the structural similarity of cyclic poly(siloxanes) to both calamitic and discotic liquid crystalline materials, these SCLC cyclic oligomers could exhibit both calamitic and discotic phases. With the appropriate structural features, these systems could exhibit transitions between calamitic and discotic phases, and therefore cross the boundaries between the optical properties of the calamitic and discotic phases. However, to our knowledge no SCLC cyclic poly(siloxane) has ever exhibited discotic (columnar) phases; the phases are all calamitic, i.e. smectic, nematic or chiral nematic.

Due to the orientation of the mesogenic group with respect to the methyl group on each of the silicon atoms, SCLC cyclic poly(siloxanes) are mixtures of stereoisomers. In the case of the SCLC cyclic siloxane tetramer there are four stereoisomers and we were the first to separate all four stereoisomers of a SCLC cyclic siloxane tetramer [10]. In earlier work on ferroelectric SCLC cyclic siloxane tetramers [11] we showed that the structure of the side chain mesogenic group plays a significant role in determining the thermal properties of the SCLC polymers. Indeed, by choosing the correct structures we were able to synthesize a number of room temperature ferroelectric SCLC cyclic tetramers, examples of which are shown in figure 1.

In this paper we describe a systematic approach to investigate the effect of molecular structure of (a) the spacer group, (b) the mesogenic side chain core and (c) the chiral end group on the thermal properties of liquid crystalline cyclic siloxane tetramers of structure 1. The difference between this present study and our previous work is that the chiral end group has been changed to a chiral ether group, with the premise that such polymers incorporating these chiral ether groups would exhibit either wider range chiral nematic or chiral SmC phases than our previous cyclic siloxane tetramers. Such polymers would be useful for either optical filters (chiral nematic phase) or ferroelectric display devices (chiral smectic C phase). The synthetic route used to prepare mesogenic monomers is given in the scheme. Details

*Author for correspondence; e-mail: D. Lacey@chem.hull.ac.uk

Liquid Crystals ISSN 0267-8292 print/ISSN 1366-5855 online © 2003 Taylor & Francis Ltd
http://www.tandf.co.uk/journals
DOI: 10.1080/0267829031000159224

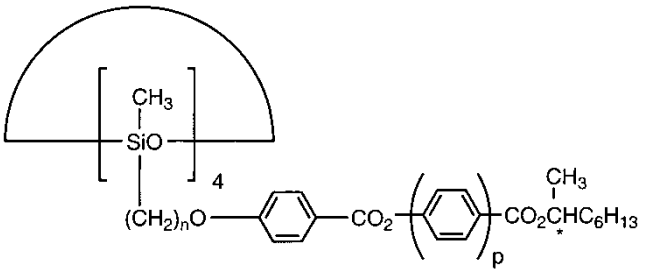

N	p	Transition temperatures
6	1	g 30.7 SmC* 47.7°C I
11	1	g 20.8 SmC* 50.5°C I
6	2	g 16.6 SmC* 117.4°C I
11	2	g 5.5 SmC* 207.8°C I

Figure 1. Transition temperatures for some room temperature ferroelectric SCLC cyclic tetramers

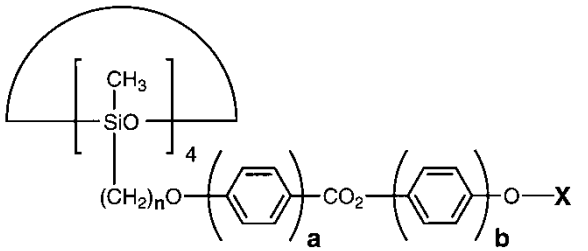

$n = 6$ or 11; $a, b = 1$ or 2

$X = CH_2CH(CH_3)C_2H_5$ (2MB) or $CH(CH_3)C_6H_{13}$ (1MH)

Structure 1.

for the preparation of the 4-alkenyloxybenzoic acids and 4-(alkenyloxy)biphenyl-4-carboxylic acids have been described previously [11].

2. Experimental

2.1. *Characterization*

^{1}H nuclear magnetic resonance spectra (NMR) were obtained using a JMN GX270FT spectrometer, using deuteriated chloroform as a solvent and tetramethylsilane as the internal standard. Infrared spectra were obtained using a Perkin Elmer 487G or a Perkin Elmer 983G spectrophotometer. Samples were prepared as either potassium bromide discs or, if liquid, were run on single crystal sodium chloride discs. Mass spectra were obtained using a Finigan 1020 GCMS spectrometer. Results are quoted where M^+ represents the molecular ion and the base peak is represented by (100%).

Optical rotational measurements were obtained using an ETL-NPL automatic polarimeter control unit Type 143A. The sample was prepared as 0.1 g of compound in 1 cm^3 of Spectrosol chloroform. Results are quoted at ambient temperature with a monochromatic sodium light source. Differential scanning calorimetry (DSC) thermograms were obtained using a Perkin-Elmer DSC 7, with a TAC 7/PC interface and a controlled cooling accessory. Heating rate was initially 20°C min^{-1}, reducing to 10°C min^{-1}. Calculations were made using Perkin Elmer UNIX-based software. The instrument was calibrated using an indium standard (m.p. 156.6°C, ΔH 28.45 J g^{-1}). Transition temperatures given in tables 1 to 4 are the onset temperatures taken from the heating cycle of the DSC traces of the tetramers. Optical microscopy was performed using an Olympus BH2 polarizing microscope, fitted with a Mettler FP52 hot stage and a Mettler FP5 controller. Samples were prepared as thin films between a glass slide and a glass cover slip.

Column chromatography was carried out under flash chromatography conditions, unless stated otherwise. The stationary phase used was Sorbsil C60 (40–60 μm). Thin layer chromatography (TLC) was carried out on aluminium sheets coated in Merck Kieselgel silica gel 60 F_{254}, eluting with dichloromethane. In the case of the carboxylic acids, ethyl acetate was used as the mobile phase. All the compounds gave a single spot by TLC. Analytical high performance liquid chromatography (HPLC) measurements were made on a reversed phase HPLC column (5 μm, 25 × 0.46 cm, Dynamax Microsorb C18 column) in conjunction with a Spectroflow 757 UV detector (254 nm) with data handling software. The mobile phase was acetonitrile. The purity of compounds **3a**–**p** was >99.5%.

Gel permeation chromatography (GPC) measurements were carried out using a Gilson refractive index detector model 131, a Kontron HPLC pump model 420 and PLgel column (5 μm, 30 × 0.75 cm mixed-C column). The column was calibrated using a series of polystyrene standards. Toluene was used as the internal standard with tetrahydrofuran (THF) as the mobile phase. All the cyclic siloxane tetramers (**C4**, **a**–**p**) were pure by GPC (100%, no trace of starting material or other comtaminants).

2.2. *Preparation of compounds* ***2(a–d)***

2.2.1. *4-[(S)-(−)-2-Methylbutyloxy]-1-benzyloxybenzene*

A solution of triphenylphosphine (7.87 g, 0.03 mol) in dry THF (50 ml) was added over 1 min to a stirred solution of 4-benzyloxyphenol (6.00 g, 0.03 mol), (*S*)-(−)-2-methyl-1-butanol (2.64 g, 0.03 mol) and diethylazodicarboxylate (5.22 g, 0.03 mol) in dry THF (100 ml), under an atmosphere of dry nitrogen. The solution was stirred overnight at room temperature and the solvent removed by distillation under reduced pressure. The

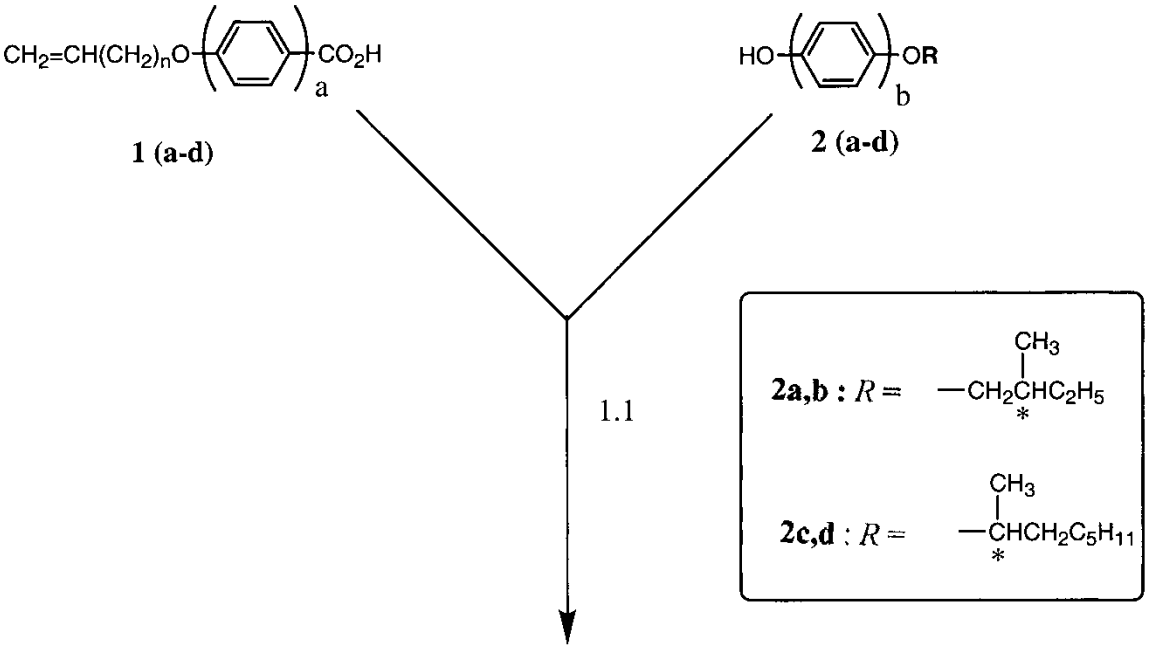

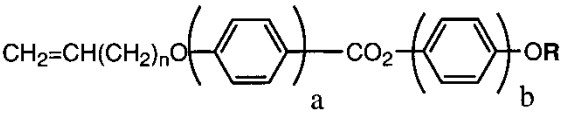

3 (a-p)

	$R =$ —CH$_2$CH(CH$_3$)C$_2$H$_5$		
	n	*a*	*b*
3a	4	1	1
3b	4	1	2
3c	4	2	1
3d	4	2	2
3e	9	1	1
3f	9	1	2
3g	9	2	1
4h	9	2	2

	$R =$ —CH(CH$_3$)CH$_2$C$_5$H$_{11}$		
	n	*a*	*b*
3i	4	1	1
3j	4	1	2
3k	4	2	1
3l	4	2	2
3m	9	1	1
3n	9	1	2
3o	9	2	1
3p	9	2	2

Scheme.
1.1: DCC, DMAP, dichloromethane.

Table 1. Structure, melting points and transition temperatures of mesogenic side chain moieties used in the preparation of the 2MB series of cyclic siloxane tetramers.

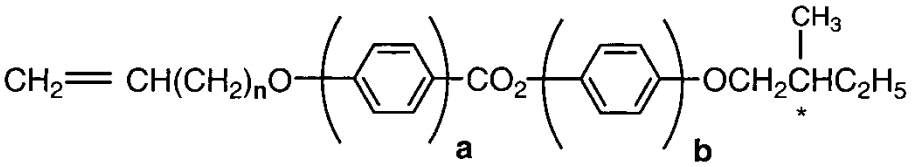

(3a-h)

Mesogenic side chain	*n*	*a*	*b*	Transition temperatures /°C
3a	4	1	1	Cr 54.8 I
3b	4	1	2	Cr 97.3 SmC* 109.2 N* 170.8 I
3c	4	2	1	Cr 115.8 SmA 192.0 I
3d	4	2	2	Cr1 147.8 Cr2 159.4 SmC* 259.9 SmA 302.7 N* 304.5 I
3e	9	1	1	Cr 47.6 SmA 56.0 I
3f	9	1	2	Cr 49.1 N* 140.7 I
3g	9	2	1	Cr 57.1 SmC* 125.9 SmA 178.1 I
3h	9	2	2	Cr 113.6 SmC* 226.1 SmA 246.6 N* 247.0 I

Table 2. Structure, melting points and transition temperatures of mesogenic side chain moieties used in the preparation of the 1MH series of cyclic siloxane tetramers.

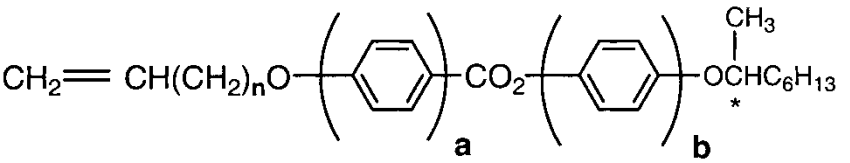

(3i-p)

Mesogenic side chain	*n*	*a*	*b*	Transition temperatures /°C
3i	4	1	1	Cr 49.1 I
3j	4	1	2	Cr 73.0 SmC* 77.9 N* 106.7 BPI 107.4 BPIII 107.8 I
3k	4	2	1	Cr 80.5 SmC* 95.4 SmA 156.6 I
3l	4	2	2	Cr 96.1 Cr2 133.3 SmC* 223.9 SmA 241.3 N* 249.7 BPI 250.3 I
3m	9	1	1	Cr 29.4 I
3n	9	1	2	Cr 71.2 SmC* 101.0 SmA 106.4 TGB_A^* 108.6 N* 114.3 BPI 116.1 I
3o	9	2	1	Cr 67.5 SmC* 87.2 SmA 132.4 I
3p	9	2	2	Cr1 93.7 Cr2 128.3 SmC* 199.2 SmA 225.0 TGB_A^* 223.3 N* 229.0 BPI 230.3 I

crude product was purified by column chromatography (dichloromethane, silica gel) to yield 4-[(*S*)-(−)-2-methylbutyloxy]-1-benzyloxybenzene as a pale yellow liquid. Yield 7.00 g (87%). ^{1}H NMR ($CDCl_3$) δ 7.35 (5H, m), 6.75 (4H, m), 5.00 (2H, s), 3.20 (2H, m), 1.95 (1H, m), 1.55 (1H, m), 1.25 (1H, m), 1.00 (6H, m). IR (KBr) ν_{max} 3080–2880, 1590, 1500, 1455, 1230 cm^{-1}. MS *m/z* 270 (M+), 198, 107, 91 (100%). $[\alpha]_D = -4.5^\circ$.

2.2.2. *4-[(R)-(+)-1-Methylheptyloxy]-1-benzyloxybenzene*

This was prepared using a similar procedure to that described in § 2.2.1. The crude product was purified by column chromatography (dichloromethane, silica gel) to yield 4-[(*R*)-(+)-1-methylheptyloxy]-1-benzyloxybenzene as a pale yellow liquid. Yield 3.54 g (75%). ^{1}H NMR ($CDCl_3$) δ 7.35 (5H, m), 6.85 (4H, m), 5.0 (2H, s), 4.2 (1H, m), 1.7 (2H, m), 1.5–1.25 (8H, m), 0.9 (3H, t).

Table 3. Structure, melting points and transition temperatures of the 2MB series of cyclic siloxane tetramers **C4**, **3a**–**h**.

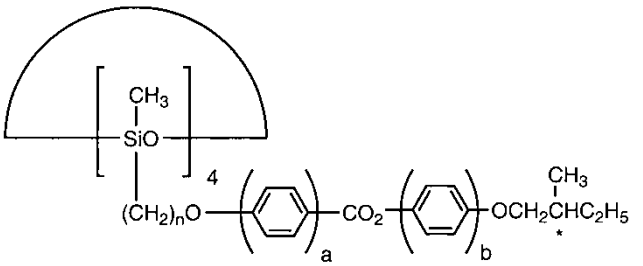

(C4, 3a-3h)

Polymer	Transition temperatures /°C
C4, **3a**	Cr 7.5 SmC* 31.0 I
C4, **3b**	Cr 74.0 SmC* 189.8 N* 198.6 I
C4, **3c**	Cr 96.2 SmC* 157.3 I
C4, **3d**	Cr1 133.6 Cr2 151.6 SmC* 277.1 SmA 285.4 N* 308.4 I
C4, **3e**	Cr 44.8 SmC* 103.1 I
C4, **3f**	Cr 70.1 N* 153.6 I
C4, **3g**	Cr1 76.7 Cr2 95.5 SmC* 209.4 I
C4, **3h**	Cr1 126.3 Cr2 146.7 SmC* 257.9 SmA 261.7 N* 277.9 I

Table 4. Structure, melting points, glass transition temperatures and transition temperatures of the 1MH series of cyclic siloxane tetramers **C4**, **3i**–**p**.

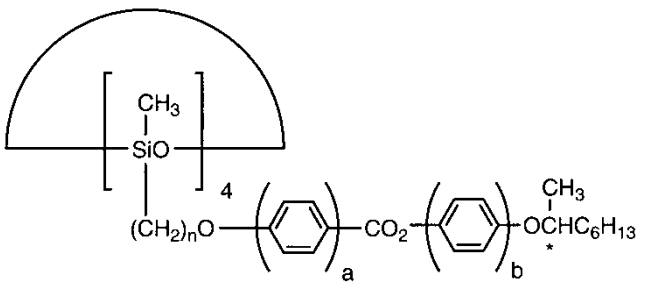

(C4, 3i-3p)

Polymer	Transition temperatures /°C
C4, **3i**	Cr 14.5 SmC* 24.7 I
C4, **3j**	Cr 31.7 SmC* 114.9 I
C4, **3k**	Cr 32.9 SmC* 140.6 I
C4, **3l**	Cr1 85.6 Cr2 124.3 SmC* 224.0 SmA 226.5 N* 241.0 I
C4, **3m**	g −22.1 SmC* 42.9 I
C4, **3n**	Cr 31.9 Cr2 45.4 SmC* 125.5 I
C4, **3o**	Cr 69.3 SmA 138.3 I
C4, **3p**	Cr1 94.6 Cr2 124.7 SmC* 202.2 SmA 225.0 N* 229.1 I

IR (KBr) ν_{max} 3000–2860, 1500, 1450, 1220, 740 cm^{-1}. MS *m/z* 312 (M+), 200, 109, 91 (100%). $[\alpha]_D = +7.8°$.

2.2.3. *(S)-(−)-4-(2-Methylbutyloxy)phenol (**2a**)*

4-[(*S*)-(−)-2-Methylbutyloxy]-1-benzyloxybenzene (6.00 g, 0.02 mol) was dissolved in 1-butanol (50 ml) and heated under reflux. Sodium metal (5.10 g, 0.20 mol) was added in small portions and the mixture heated under reflux for 30 min until all the sodium metal had reacted. The solution was allowed to cool completely and water (15 ml) was carefully added followed by dilute hydrochloric acid (15 ml, 20%). The product was extracted into diethyl ether (150 ml) and the organic phase separated, washed with saturated sodium chloride solution (50 ml), water (50 ml) and then dried ($MgSO_4$). The solvent was then removed by distillation under reduced pressure to yield compound **2a** as a yellow liquid. Yield 3.40 g (71%). ^{1}H NMR ($CDCl_3$) δ 7.40 (2H, m), 6.85 (2H, m), 5.00 (1H, s), 3.60 (2H, m), 1.85 (1H, m), 1.55 (1H, m), 1.25 (1H, m), 1.0 (6H, m). IR (KBr) ν_{max} 3500, 3180, 1590, 1500, 1455, 1380, 1220 cm^{-1}. MS *m/z* 180 (M+), 109 (100%), 93, 81, 65, 55. $[\alpha]_D = -3.6°$.

2.2.4. *(R)-(+)-4-(1-Methylheptyloxy)phenol (**2c**)*

This was prepared using a similar procedure to that outlined for the preparation of compound **2a**. Yield 1.50 g (50%, yellow liquid). ^{1}H NMR ($CDCl_3$) δ 6.75 (4H, m), 4.6 (1H, s), 4.15 (1H, m), 1.7 (2H, m), 1.6–1.2 (8H, m), 0.9 (3H, m). IR (KBr) ν_{max} 3540–3100, 2880–2860, 1500, 1450, 1230, 1120, 1100, 840 cm^{-1}. MS *m/z* 222 (M+), 110 (100%), 91, 81, 65, 55. $[\alpha]_D = +6.4°$.

2.2.5. *4-(Methoxycarbonyloxy)-4′-hydroxybiphenyl*

4-4′-Biphenol (15.00 g, 0.08 mol) was added, with stirring, to a solution of sodium hydroxide (4.80 g, 0.18 mol) in water (200 ml) at 0°C. Methyl chloroformate (3.80 g, 0.12 mol) was added slowly to the suspension and the temperature maintained at 0°C. The mixture was stirred for 4 h at room temperature and then brought to pH 4–5 by the addition of a mixture of concentrated hydrochloric acid and water (1:1). The voluminous precipitate was filtered off and washed with water. Recrystallization (ethanol) afforded 4-(methoxycarbonyloxy)-4′-hydroxybiphenyl as a white powder. Yield 4.80 g (49%). ^{1}H NMR ($CDCl_3$) δ 7.55 (2H, m), 7.45 (2H, m), 7.25 (2H, m), 6.85 (2H, m), 4.9 (1H, s), 3.95 (3H, s). IR (KBr) ν_{max} 3500–3400, 3080–2980, 1740, 1610, 1590, 1500, 1440, 1290, 1210 cm^{-1}. MS *m/z* 243 (M+), 199 (100%), 185.

2.2.6. *(R)-(+)-4-(1-Methylheptyloxy)-4′-(methoxycarbonyloxy)biphenyl*

This was prepared using a similar procedure to that described is §2.2.5. Yield 1.20 g (28%, white solid). ^{1}H NMR ($CDCl_3$) δ 7.55 (2H, d), 7.45 (2H, d), 7.25 (2H, d), 6.95 (2H, d), 4.40 (1H, m), 3.90 (3H, s), 1.75–1.30 (10H, m), 0.90 (3H, t). IR (KBr) ν_{max} 3040–2860, 1760, 1600, 1490, 1440, 1260, 1220, 820 cm^{-1}. MS *m/z* 356 (M+), 303, 244, 199, 171, 128, 71, 59 (100%), 43. $[\alpha]_D = +9.5^\circ$.

2.2.7. *(R)-(+)-4-(1-Methylheptyloxy)-4′-hydroxybiphenyl (**2d**)*

(*R*)-(+)-4-(1-Methylheptyloxy)-4′-(methoxycarbonyloxy)biphenyl (1.20 g, 3.37 mmol) was added to a mixture of ethanol (75 ml) and ammonia (25 ml) and stirred for 4 h at room temperature. The solvent was removed by distillation at room temperature. Ether (100 ml) was added to the residue and the ethereal solution was washed with saturated sodium hydrogen carbonate (3 × 50 ml), water (2 × 50 ml) and dried ($MgSO_4$). The ether was removed by distillation under reduced pressure to afford compound **2d** as a white solid. Yield 1.00 g (100%), m.p. 153–154°C. ^{1}H NMR ($CDCl_3$) δ 7.44 (2H, d), 7.42 (2H, d), 6.92 (2H, d), 6.88 (2H, d), 4.70 (1H, s), 4.40 (1H, m), 1.75 (2H, m), 1.60–1.25 (8H, m), 0.90 (3H, t). IR (KBr) ν_{max} 3600–3200, 1600, 1500, 1240, 820 cm^{-1}. MS *m/z* 298 (M+), 186 (100%). $[\alpha]_D = +9.3^\circ$.

2.2.8. *(S)-(−)-4-(2-Methylbutyloxy)-4′-hydroxybiphenyl (**2b**)*

This was prepared using a similar procedure to that outlined for the preparation of compound **2d**. Yield 6.30 g (43%), white solid, m.p. 158–159°C. ^{1}H NMR ($CDCl_3$) δ 7.45 (2H, d), 7.40 (2H, d), 6.95 (2H, d), 6.90 (2H, d), 5.60 (1H, s), 3.80 (2H, m), 1.85 (1H, m), 1.60 (1H, m), 1.30 (1H, m), 0.95 (6H, m). IR (KBr) ν_{max} 3400–3200, 3000–2840, 1600, 1500, 1240, 1160, 820 cm^{-1}. MS *m/z* 256 (M+), 185 (100%), 169, 157, 65, 55. $[\alpha]_D = -7.6^\circ$.

2.3. *Preparation of mesogenic side-chains **3**(**a**–**p**)*

2.3.1. *(S)-(−)-4-(2-Methylbutyloxy)phenyl 4-(hex-5-enyloxy)benzoate (**3a**)*

The following preparation of compound **3a** exemplifies the method used to prepare compounds **3b**–**p**. 4-(Hex-5-enyloxy)benzoic acid (1.10 g, 5.00 mmol), (*S*)-(−)-4-(2-methylbutyloxy)phenol (**2b**) (1.00 g, 5.56 mmol) and dimethylaminopyridine (0.07 g, 0.56 mmol) were dissolved in dry dichloromethane (150 ml) under anhydrous conditions. N,N′-Dicyclohexylcarbodiimide (1.14 g, 5.56 mmol) in dry dichloromethane (20 ml) was added and the reaction mixture stirred at room temperature overnight. The precipitated (DCU) was filtered off and the solvent removed by distillation under reduced pressure. The crude ester was then purified by flash column chromatography (dichloromethane, silica gel) and recrystallized (acetonitrile) to afford compound **3a** as a white crystalline solid. Yield 0.65 g (35%), m.p. 54.8°C. ^{1}H NMR ($CDCl_3$) δ 8.13 (2H, d), 7.10 (2H, d), 6.96 (2H, d), 6.92 (2H, d), 5.84 (2H, m), 5.03 (1H, m), 4.05 (2H, t), 3.78 (2H, m), 2.15 (2H, m), 1.85 (2H, m), 1.60 (3H, m), 1.26 (2H, m), 0.98 (6H, m). IR (KBr) ν_{max} 3075, 2960, 2930, 2880, 2860, 1740, 1600, 1510, 1280, 1250, 1200, 1180, 1070, 760 cm^{-1}. MS *m/z* 382 (M+), 334, 221, 203 (100%), 179, 161, 138, 121(100%), 109, 93. $[\alpha]_D = -3.0^\circ$.

2.3.2. *(S)-(−)-4′-(2-Methylbutyloxy)biphenyl 4′-(hex-5-enyloxy)benzoate (**3b**)*

Yield 1.14 g (64%), Cr 97.3 SmC* 109.2 N* 170.8 I (°C). ^{1}H NMR ($CDCl_3$) δ 8.16 (2H, d), 7.59 (2H, d), 7.50 (2H, d), 7.25 (2H, d), 7.00 (4H, m), 5.85 (2H, m), 5.00 (1H, m), 4.10 (2H, t), 3.85 (2H, m), 2.15 (2H, m), 1.85 (4H, m), 1.60 (2H, m), 1.35 (1H, m), 1.00 (6H, m). IR (KBr) ν_{max} 3080–2820, 1720, 1600, 1290 760 cm^{-1}. MS *m/z* 458 (M+), 446, 432, 404, 390, 377, 256, 203 (100%), 185, 157, 139, 128, 121, 115, 104, 93, 65. $[\alpha]_D = -7.6^\circ$.

2.3.3. *(S)-(−)-4-(2-Methylbutyloxy)phenyl 4-(hex-5-enyloxy)biphenyl-4-carboxylate (**3c**)*

Yield 1.34 g (62%), Cr 115.8 SmA 192.0 I (°C). ^{1}H NMR ($CDCl_3$) δ 8.24 (2H, d), 7.69 (2H, d), 7.60 (2H, d), 7.13 (2H, d), 7.00 (2H, d), 6.94 (2H, d), 5.85 (2H, m), 5.05 (1H, m), 4.05 (2H, t), 3.80 (2H, m), 2.15 (2H, m), 1.85 (4H, m), 1.55 (2H, m), 1.35 (1H, m), 0.95 (6H, m). IR (KBr) ν_{max} 3080–2820, 1720, 1600, 1290 760 cm^{-1}. MS *m/z* 458 (M+), 279 (100%), 197, 168, 151, 141, 109, 65, 55. $[\alpha]_D = -5.8^\circ$.

2.3.4. *(S)-(−)-4′-(2-Methylbutyloxy)biphenyl 4′-(hex-5-enyloxy)biphenyl-4-carboxylate (**3d**)*

Yield 0.66 g (45%), Cr_1 147.8 Cr_2 159.4 SmC* 259.9 SmA 302.7 N* 304.5 I (°C). ^{1}H NMR ($CDCl_3$) δ 8.26 (2H, d), 7.70 (2H, d), 7.62 (2H, d), 7.58 (2H, d), 7.53 (2H, d), 7.28 (2H, d), 7.03 (2H, d), 6.98 (2H, d), 5.85 (2H, m), 5.00 (1H, m), 4.05 (2H, t), 3.82 (2H, m), 2.15 (2H, m), 1.85 (4H, m), 1.55 (2H, m), 1.35 (1H, m), 1.00 (6H, m). IR (KBr) ν_{max} 3080–2840, 1720, 1600, 1290, 760 cm^{-1}. MS *m/z* 534 (M+), 523, 509, 469, 454, 349, 296, 290 (100%), 196, 185, 169, 141, 115, 55, 43. $[\alpha]_D = -3.7^\circ$.

2.3.5. *(S)-(−)-4-(2-Methylbutyloxy)phenyl 4-(undec-10-enyloxy)benzoate (**3e**)*

Yield 0.6 g (27%), Cr 47.6 SmA 56.0 I (°C). ^{1}H NMR ($CDCl_3$) δ 8.13 (2H, d), 7.10 (2H, d), 6.96 (2H, d), 6.92 (2H, d), 5.82 (2H, m), 4.97 (1H, m), 4.04 (2H, t), 3.78 (2H, m), 2.05 (2H, m), 1.83 (2H, m), 1.65–1.21 (16H, m), 0.99 (6H, m). IR (KBr) ν_{max} 3080, 2960, 2920, 2850, 1740, 1600, 1510, 1460, 1280, 1250, 1200, 1170, 1075, 760 cm^{-1} MS *m/z* 452 (M+), 351, 274, 232, 196, 147, 133, 121 (100%), 110. 93, 65. $[\alpha]_D = -6.0°$.

2.3.6. *(S)-(−)-4-(2-Methylbutyloxy)biphenyl 4′-(undec-10-enyloxy)benzoate (**3f**)*

Yield 0.65 g (32%), Cr 49.1 N* 140.7 I (°C). ^{1}H NMR ($CDCl_3$) δ 8.15 (2H, d), 7.65 (2H, d), 7.60 (2H, d), 7.15 (2H, d), 7.00 (2H, d), 6.95 (2H, d), 5.80 (2H, m), 4.95 (1H, m), 4.00 (2H, t), 3.80 (2H, m), 2.05 (2H, m), 1.85 (4H, m), 1.60–1.20 (16H, m), 1.00 (6H, m). IR (KBr) ν_{max} 3000–2859, 1730, 1600, 1500, 1520, 1210, 1170 cm^{-1}. MS *m/z* 528 (M+), 273, 255, 185, 121 (100%). $[\alpha]_D = -3.5°$.

2.3.7. *(S)-(−)-4-(2-Methylbutyloxy)phenyl 4′-(undec-10-enyloxy)biphenyl-4-carboxylate (**3g**)*

Yield 0.70 g (44%), Cr 57.1 SmC* 125.9 SmA 178.1 I (°C). ^{1}H NMR ($CDCl_3$) δ 8.23 (2H, d), 7.68 (2H, d), 7.59 (2H, d), 7.12 (2H, d), 7.00 (2H, d), 6.93 (2H, d), 5.83 (2H, m), 5.00 (1H, m), 4.00 (2H, t), 3.80 (2H, m), 2.05 (2H, m), 1.85 (4H, m), 1.60–1.20 (16H, m), 1.00 (6H, m). IR (KBr) ν_{max} 3040–2800, 1740, 1600, 1500, 1250, 1200, 1160 cm^{-1}. MS *m/z* 528 (M+), 487, 471, 349 (100%) 196, 168, 141, 121. $[\alpha]_D = -9.6°$.

2.3.8. *(S)-(−)-4′-(2-Methylbutyloxy)biphenyl 4-(undec-10-enyloxy)biphenyl-4-carboxylate (**3h**)*

Yield 0.50 g (38%), Cr 113.6 SmC* 226.1 SmA 246.6 N* 247.0 I (°C). ^{1}H NMR ($CDCl_3$) δ 8.26 (2H, d), 7.71 (2H, d), 7.61 (2H, d), 7.98 (2H, d), 7.52 (2H, d), 7.28 (2H, d), 7.02 (2H, d), 6.98 (2H, d), 5.85 (2H, m), 5.00 (1H, m), 4.05 (2H, t), 3.85 (2H, m), 2.10 (2H, m), 1.85 (4H, m), 1.60–1.20 (16H, m), 1.00 (6H, m). IR (KBr) ν_{max} 3100–2880, 1730, 1600, 1500, 1280, 1200, 1060 cm^{-1}. MS *m/z* 604 (M+), 466, 349 (100%), 273, 225, 211, 57. $[\alpha]_D = -3.5°$.

2.3.9. *(R)-(+)-4-(1-Methylheptyloxy)phenyl 4-(hex-5-enyloxy)benzoate (**3i**)*

Yield 0.66 g (39%), m.p. 41.9°C. ^{1}H NMR ($CDCl_3$) δ 8.12 (2H, d), 7.11 (2H, d), 6.98 (2H, d), 6.90 (2H, d), 5.84 (2H, m), 5.02 (1H, m), 4.32 (1H, m), 4.04 (2H, t), 2.30 (2H, m), 1.82 (2H, m), 1.63 (2H, m), 1.48–1.35 (13H, m), 0.85 (3H, m). IR (KBr) ν_{max} 3080, 2960, 2920, 2860, 1740, 1600, 1500, 1460, 1280, 1195, 1170, 1070, 760 cm^{-1}. MS *m/z* 424 (M+), 413, 357, 340, 313, 245, 203, 161, 147, 121 (100%), 104, 93, 71, 65, 55, 43. $[\alpha]_D = +5.0°$.

2.3.10. *(R)-(+)-4′-(1-Methylheptyloxy)biphenyl 4′-(hex-5-enyloxy)benzoate (**3j**)*

Yield 1.32 g (78%), Cr 73.0 SmC* 77.9 N* 107.0 BP1 107.4 BP2 107.8 I (°C). ^{1}H NMR ($CDCl_3$) δ 8.17 (2H, d), 7.58 (2H, d), 7.49 (2H, d), 7.24 (2H, d), 6.98 (2H, d), 6.94 (2H, d), 5.85 (2H, m), 5.00 (1H, m), 4.35 (1H, m), 4.05 (2H, t), 2.15 (2H, m), 1.85 (2H, m), 1.60 (2H, m), 1.50–1.30 (13H, m), 0.90 (3H, m). IR (KBr) ν_{max} 3000–2820, 1720, 1600, 1500. 1490, 1270, 1250, 1220 cm^{-1}. MS *m/z* 500 (M+), 388, 349, 298, 203 (100%), 185, 157, 121, 93, 65, 55. $[\alpha]_D = +3.8°$.

2.3.11. *(R)-(+)-4-(1-Methylheptyloxy)phenyl 4′-(hex-5-enyloxy)biphenyl-4-carboxylate (**3k**)*

Yield 1.58 g (62%), Cr 80.5 SmC* 95.4 SmA 156.5 I (°C). ^{1}H NMR ($CDCl_3$) δ 8.23 (2H, d), 7.68 (2H, d), 7.59 (2H, d), 7.12 (2H, d), 7.01 (2H, d), 6.93 (2H, d), 5.85 (2H, m), 5.00 (1H, m), 4.35 (1H, m), 4.05 (2H, t), 2.15 (2H, m), 1.85 (2H, m), 1.60 (2H, m), 1.50–1.30 (13H, m), 0.90 (3H, m). IR (KBr) ν_{max} 3010–2830, 1730, 1600, 1500. 1490, 1270, 1250, 1220 cm^{-1}. MS *m/z* 500 (M+), 432, 388, 349, 279 (100%), 211, 197, 169, 141, 121, 109, 55. $[\alpha]_D = +3.6°$.

2.3.12. *(R)-(+)-4′-(1-Methylheptyloxy)biphenyl 4′-(hex-5-enyloxy)biphenyl-4-carboxylate (**3l**)*

Yield 0.14 g (16%), Cr_1 96.1 Cr_2 133.3 SmC* 223.9 SmA 241.3 N* 249.7 BP1 250.3 I (°C). ^{1}H NMR ($CDCl_3$) δ 8.26 (2H, d), 7.70 (2H, d), 7.62 (2H, d), 7.59 (2H, d), 7.51 (2H, d), 7.28 (2H, d), 7.02 (2H, d), 6.97 (2H, d), 5.85 (2H, m), 5.02 (1H, m), 4.40 (1H, m), 4.04 (2H, t), 2.15 (2H, m), 1.84 (2H, m), 1.60 (2H, m), 1.38–1.24 (13H, m), 0.90 (3H, m). IR (KBr) ν_{max} 3080, 2920, 2880, 1740, 1600, 1490, 1270, 1250, 1210, 1130, 760 cm^{-1}. MS *m/z* 576 (M+), 573, 567, 561, 512, 468, 397, 280 (100%), 211, 197, 185, 170, 141. 115. $[\alpha]_D = +7.1°$.

2.3.13. *(R)-(+)-4-(1-Methylheptyloxy)phenyl 4′-(undec-10-enyloxy)benzoate (**3m**)*

Yield 1.22 g (55%), m.p. 29.4°C. ^{1}H NMR ($CDCl_3$) δ 8.13 (2H, d), 8.11 (2H, d), 7.35 (2H, d), 6.95 (2H, d), 5.15 (2H, m), 4.95 (1H, m), 4.00 (2H, t), 2.10 (2H, m), 1.85 (4H, m), 1.50–1.20 (23H, m), 0.90 (3H, m). IR (KBr) ν_{max} 3000–2820, 1720, 1600, 1500, 1260, 1210, 1160 cm^{-1}. MS *m/z* 494 (M+), 482, 414, 396, 274 (100%), 161, 149, 133, 121, 107, 92, 65, 55. $[\alpha]_D = +8.4°$.

2.3.14. *(R)-(+)-4′-(1-Methylheptyloxy)biphenyl 4′-(undec-10-enyloxy)benzoate (**3n**)*

Yield 1.11 g (58%), Cr 71.2 SmC* 101.0 SmA 106.4 TGB_A^* 108.6 N* 114.3 BP1 116.1 I (°C). ^{1}H NMR ($CDCl_3$) δ 8.15 (2H, d), 7.60 (2H, d), 7.55 (2H, d), 7.35 (2H, d), 6.98 (2H, d), 6.95 (2H, d), 5.80 (2H, m), 4.95 (1H, m), 4.40 (1H, m), 4.00 (2H, t), 2.10 (2H, m), 1.35 (4H, m), 1.60–1.25 (23H, m), 0.85 (3H, m). IR (KBr) ν_{max} 3000–2800, 1720, 1600, 1500, 1270, 1210, 1180, 1070 cm^{-1}. MS *m/z* 570 (M+), 298, 273, 185, 121(100%), 55. $[\alpha]_D = +3.1°$.

2.3.15. *(R)-(+)-4-(1-Methylheptyloxy)phenyl 4′-(undec-10-enyloxy)biphenyl-4-carboxylate (**3o**)*

Yield 0.30 g (20%), Cr 67.5 SmC* 87.2 SmA 132.4 I (°C). ^{1}H NMR ($CDCl_3$) δ 8.23 (2H, d), 7.69 (2H, d), 7.59 (2H, d), 7.12 (2H, d), 7.01 (2H, d), 6.92 (2H, d), 5.83 (2H, m), 4.95 (1H, m), 4.34 (1H, m), 4.02 (2H, t), 2.05 (2H, m), 1.80 (4H, m), 1.61–1.20 (23H, m), 0.89 (3H, m). IR (KBr) ν_{max} 2920, 2850, 1720, 1600, 1500, 1470, 1440, 1280, 1170, 1080, 840, 760 cm^{-1}. MS *m/z* 570 (M+), 350 (100%), 307, 197, 169, 141, 110, 81, 69, 55. $[\alpha]_D = +6.7°$.

2.3.16. *(R)-(+)-4′-(1-Methylheptyloxy)biphenyl 4′-(undec-10-enyloxy)biphenylcarboxylate (**3p**)*

Yield 1.16 g (54%), Cr_1 93.7 Cr_2 128.3 SmC* 199.2 SmA 225.0 TGB_A^* 223.3 N* 229.0 BP 230.3 I (°C). ^{1}H NMR ($CDCl_3$) δ 8.25 (2H, d), 7.70 (2H, d), 7.60 (2H, d), 7.51 (2H, d), 7.27 (2H, d), 7.00 (2H, d), 6.96 (2H, d), 5.80 (2H, m), 4.95 (1H, m), 4.40 (1H, m), 4.00 (2H, t), 2.10 (2H, m), 1.35 (4H, m), 1.60–1.25 (23H, m), 0.85 (3H, m). IR (KBr) ν_{max} 3000–2810, 1720, 1600, 1500, 1250, 1220, 1190, 1070 cm^{-1}. MS *m/z* 646 (M+), 349 (100%), 307, 225, 203, 197, 186, 169, 141, 121, 69, 55. $[\alpha]_D = +2.2°$.

2.4. *Preparation of the cyclic siloxane tetramers*

Full experimental details of the hydrosilylation reaction used to prepare the cyclic siloxane tetramers are given in reference [11]. The amounts of poly(siloxane) backbone and mesogenic side chain precursor used and yields for the hydrosylylation reaction are given in tables 5 and 6.

The ^{1}H NMR data for these tetramers are not shown individually. All polymers show similar ^{1}H NMR traces to the mesogenic side group with the loss of the alkenic protons $\delta = 5.85$ and $\delta = 5.00$, and include an extra signal for the methyl protons attached to the ring, $\delta = 0.10$.

Table 5. The quantities of poly(siloxane) backbone and mesogenic side chain precursor used and yields for the preparation of cyclic siloxane tetramers **C4**, **3a**–**h**.

Tetramer	Cyclic backbone/g	Mesogen/g	Yield/g(%)
C4, **3a**	0.040	0.30	0.05 (16)
C4, **3b**	0.060	0.50	0.51 (90)
C4, **3c**	0.041	0.35	0.10 (28)
C4, **3d**	0.030	0.30	0.26 (87)
C4, **3e**	0.030	0.25	0.14 (55)
C4, **3f**	0.021	0.20	0.04 (20)
C4, **3g**	0.032	0.30	0.12 (40)
C4, **3h**	0.013	0.15	0.12 (80)

Table 6. The quantities of poly(siloxane) backbone and mesogenic side chain precursor used and yields for the preparation of cyclic siloxane tetramers **C4**, **3i**–**p**.

Tetramer	Cyclic backbone/g	Mesogen/g	Yield/g(%)
C4, **3i**	0.019	0.15	0.08 (50)
C4, **3j**	0.065	0.60	0.25 (41)
C4, **3k**	0.065	0.60	0.26 (43)
C4, **3l**	0.005	0.05	0.03 (75)
C4, **3m**	0.055	0.50	0.22 (11)
C4, **3n**	0.047	0.50	0.28 (14)
C4, **3o**	0.010	0.10	0.07 (70)
C4, **3p**	0.042	0.50	0.25 (13)

3. Results and Discussion

The results from this investigation on liquid crystalline (LC) cyclic siloxane tetramers can be conveniently divided into two sections. Section 3.1 details the effect of molecular structure of the monomeric mesogenic side chain on their LC behaviour whilst a similar, but more detailed, study on their corresponding cyclic siloxane tetramers is outlined in § 3.2.

3.1. *Monomeric mesogenic side chains*

A schematic representation of the structure of the mesogenic side chain used in this study is given in figure 2, which clearly shows its three different features that will be used to investigate the role of molecular structure on their thermal properties. The results from our work on the monomeric mesogenic side chains are subdivided into two sections, depending on the structure of the chiral end group used.

3.1.1. *The 2MB series*

The structure, melting points and transition temperatures of the mesogenic side chain moieties used in the preparation of the 2MB series of cyclic siloxane tetramers are given in table 1. All the compounds in the 2MB Series contain the (*S*)-(−)-2-methylbutyl (2MB) chiral end group. All the mesogenic side chains (**4a**–**h**) contain a terminally positioned alkenyl group that was

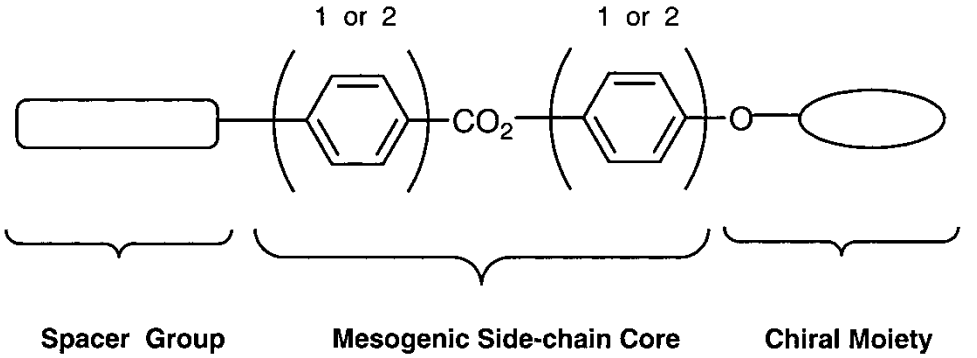

Figure 2. A schematic representation of the structure of the mesogenic side chain used in this study.

used to attach the side chain to the cyclic tetramer backbone. They therefore have an effective spacer group length of 6 ($n=4$) or 11 ($n=9$) carbon atoms.

3.1.1.1. *Compounds with a short spacer group ($n=4$).* Compound **3a** is the only compound in this series that does not appear to exhibit liquid crystalline phases. The addition of a further phenyl ring in the core near to the chiral end group, compound **3b**, gave a marked increase of melting point and liquid crystalline behaviour, with **3b** exhibiting SmC* and N* phases. This is in contrast to **3c** where the introduction of an additional phenyl ring near to the spacer group led to the formation of the SmA phase. Both the melting and clearing points for **3c** are much higher than those found for **3b**. In the case of compound **3d**, where we have two phenyl rings either side of the ester group, this four-ring compound has the highest melting point of all the four compounds studied and exhibits all the phases associated with **3b** and **3c**, i.e. SmA, SmC* and N*.

3.1.1.2. *Compounds with a long spacer group ($n=9$).* Unlike the compounds with short spacer groups, all these with long spacer groups exhibited liquid crystalline behaviour. Compounds **3f**, **3g** and **3h** had substantially lower melting points than the corresponding compound with a shorter spacer group, some 45–60°C lower; but the introduction of the longer spacer group dramatically decreased their clearing points by as much as 50°C in the case of **3h**. Again, as with the series of compounds with a shorter spacer group, we see a marked change in liquid crystalline behaviour (**3f** and **3g**) with respect to the position of the additional third phenyl ring. In the case of compound **3f**, where the additional phenyl ring was placed near to the chiral end group, a N* phase is observed, but if this additional ring is placed near to the spacer group, as in **3g**, we observe SmA and SmC* phases. Although this is slightly different from the previous compounds with shorter spacer groups it does seem that, in general, the incorporation of a third phenyl ring next to the chiral end group favours the formation of the N* phase. Positioning the third phenyl ring near to the spacer group is conducive to the formation of smectic phases. Compound **3h**, the four-ring compound, exhibits the same types of phases as the corresponding shorter spacer group compound **3d**, i.e. SmA, SmC* and N* phases, but with reduced transition temperatures.

3.1.2. *The 1MH Series*

The structure, melting points and transition temperatures of the mesogenic side chain moieties used in the preparation of the 1MH series of cyclic siloxane tetramers are given in table 2. All the compounds in the 1MH series contain the (*R*)-(+)-1-methylheptyl (1MH) chiral end group. For compounds containing a short spacer group the most significant change in the thermal properties of these compounds was observed by changing the end chiral group from (*S*)-(−)-2-methylbutyl to (*R*)-(+)-1-methylheptyl. This dramatically decreased both the melting points and thermal stability of the mesophases exhibited by these compounds. For example, in the case of compound **3l** the melting point was decreased by 51.7°C, the SmC* thermal stability by 36.0°C, the SmA thermal stability by 61.4°C and the chiral nematic thermal stability by 54.8°C.

The decrease in the melting points and transition temperatures of the mesophases was also observed for the compounds containing the longer spacer group ($n=9$), although the decrease is far less dramatic than that observed for the shorter spacer group compounds, **3i** to **3l**. For example, in the case of compound **3p**, which is analogous to compound **3l**, the decrease in its melting point was 19.9°C, and the decreases in the thermal stability of the mesophases were SmC* 26.9°C,

SmA 21.6°C and the chiral nematic phase 18.0°C. However, the most significant change in the liquid crystalline behaviour of these compounds was the appearance of the TGB_A^* phase for compounds **3n** and **3p**. The TGB phase is typically observed at the transition between the isotropic liquid or chiral nematic phase to the SmA (TGBA) or SmC (TGBC) phases. At the N* to SmA or SmC transition the helical arrangement of the chiral nematic gives way to the layered structure of the SmA or SmC phases. However, in some cases there is competition between molecules forming a helical structure, due to the presence of the chiral moiety in their structure, and the formation of a lamellar structure, which is indicative of the smectic A and C phases. These two structures are incompatible and cannot coexist without forming defects. This antagonistic situation between helical and lamellar formation is resolved by the appearance of a periodic ordering of screw dislocations which enable helical/lamellar structures to coexist. This results in the formation of the twist grain boundary phases that are composed of small lamellar SmA or SmC domains arranged to form a macroscopic helical structure. This phase is relatively rare in liquid crystalline materials and in many cases only exists over a few degrees. For compounds **3n** and **3p** the TGB_A^* range is only 5.7°C.

3.2. *Liquid crystalline cyclic siloxane tetramers*

3.2.1. *Explanation of nomenclature*

The following nomenclature has been used for the identification of cyclic siloxane tetramers prepared in this study. Reference to the mesogenic side chain is made at all times to allow for ease of cross-reference. All cyclic siloxane tetramers are designated as **C*n*,*yy***. Here **C** refers to the cyclic backbone; ***n*** number of silicon atoms in the ring, e.g. 4 for the cyclic tetramers; and ***yy*** is the mesogenic side chain (see tables 1 and 2 for structure). Thus, **C4**, **3a** is used to refer to structure 2.

As in the section on monomeric mesogenic side chains, the discussion of the results regarding the cyclic siloxane tetramers can be divided into two sections depending on the structure of the chiral end group.

3.2.2. *Cyclic siloxane tetramers incorporating mesogenic side chains containing the chiral (S)-(−)-2-methylbutyl end group; the MB series*

The structure and transition temperatures for these cyclic siloxane tetramers are given in table 3. All the cyclic tetramers exhibited liquid crystalline behaviour and a crystal to mesophase transition (melting point); none exhibited a glass transition temperature. In the case where the cyclic tetramer contained a short spacer group (compounds **C4**, **3a** to **C4**, **3d**), melting points were lower than those found for the corresponding monomeric mesogenic side chains (**3a** to **3d**). However, with the exception of cyclic tetramer **C4**, **3e**, the cyclic tetramers with the longer spacer group gave higher melting points than their monomeric mesogenic side chain counterparts (**3f** to **3h**). The cyclic tetramer **C4**, **3e** was very unusual in that it had a very low melting point and exhibited a very low SmC*–I transition, far lower than we would have anticipated from the results given in table 1. All the polymers exhibited the same type of phases as their monomeric mesogenic side chain counterparts, i.e. SmA, SmC* and N* phases.

A detailed summary of the effects of (a) the length of the spacer group, (b) the arrangement of the phenyl rings in the mesogenic side chain core and (c) the structure of the chiral end group on the liquid crystalline thermal properties of the cyclic siloxane tetramers is given later.

3.2.3. *Cyclic siloxane tetramers incorporating mesogenic side chains containing the chiral (R)-(+)-1-methylheptyl end group; the MH series*

The structure and transition temperatures for these cyclic siloxane tetramers are given in table 4. All the cyclic tetramers exhibited liquid crystalline behaviour and with the exception of **C4**, **3m**, gave crystal to mesophase transitions (melting points). The cyclic tetramer **C4**, **3m** was the only one in either series of tetramers to exhibit a glass transition temperature. Unlike the previous series only the cyclic tetramer **C4**, **3o** had a melting point higher than its monomeric side chain counterpart; all the other cyclic tetramers had lower melting points. The melting points for the MH series of

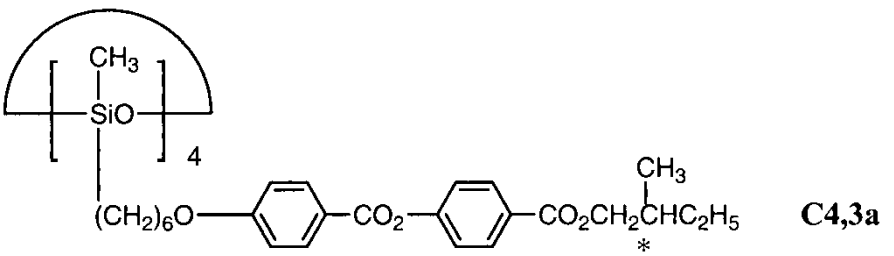

Structure 2.

cyclic tetramers were much lower than the corresponding members of the MB series, typically 30–60°C lower. The only exception was the cyclic tetramer **C4**, **3a** which has a lower melting point than tetramer **C4**, **3i**. This highlights, again, the unusually low melting point found for tetramer **C4**, **3a**. All the tetramers were clean and highly pure and therefore this melting point anomaly was not caused by contamination.

3.3. *Liquid crystalline behaviour*

A detailed summary of the effects of (a) the arrangement of the phenyl rings in the mesogenic side chain core, (b) the length of the spacer group, and (c) the structure of the chiral end group on the liquid crystalline thermal properties of the cyclic siloxane tetramers is now given.

3.3.1. *The effect of the number and arrangement of the phenyl rings in the mesogenic side chain on SmC* thermal stability and range*

The meaning of the terms *X*, *n*, *a* and *b* used throughout this discussion can be found by reference to structure 1. Relative stability of the SmC* phase is given in table 7. It must be remembered that out of the 16 cyclic tetramers synthesized only **C4**, **3f** (N*) and **C4**, **3o** (SmA) did not exhibit a ferroelectric SmC* phase. The difference in SmC* thermal stability between the MB and MH series of cyclic tetramers was very varied. In some cases the difference was very small, e.g. the difference between compounds **C4**, **3a** and **C4**, **3I** was only 6.3°C but between **C4**, **3b** and **C4**, **3j** the difference was 74.9°C.

3.3.2. *The effect of the length of the spacer group on SmC* thermal stability and glass/crystalline transition temperatures*

For a given chiral end group, the effect of the spacer group length depended greatly on the arrangement of the phenyl rings in the mesogenic side chain. For cyclic siloxane tetramers containing the 2MB chiral end group, the SmC* thermal stability for the spacer group $n=6>n=11$, for tetramers where the ratio a:b=1:2 and 2:2, but is reversed, i.e. $n=11>n=6$, for tetramers where the ratio a:b=1:1 and 2:1. For cyclic siloxane tetramers containing the 1MH chiral end group, the SmC* thermal stability for the spacer group $n=6>n=11$, for tetramers where the ratio a:b=2:1 and 2:2, but again is reversed, i.e. spacer group $n=11>n=6$, for tetramers where the ratio a:b=1:1 and 1:2.

Table 7. Relative stability of SmC* phase.

X	*n*	Relative stability of SmC* relative to *a*:*b*
$CH_2CH^*(CH_3)C_2H_6$	6	2:2 > 1:2 > 2:1 > 1:1
$CH_2CH^*(CH_3)C_2H_6$	11	2:2 > 2:1 > 1:1 > 1:2 (N*)
$CH^*C_6H_{13}$	6	2:2 > 2:1 > 1:2 > 1:1 (SmA)
$CH^*C_6H_{13}$	11	2:2 > 2:1 > 1:2 > 1:1

For cyclic siloxane tetramers containing the 2MB chiral end group the glass or crystalline transition temperatures for spacer group $n=6>n=11$, except when a:b=1:1; while for cyclic siloxane tetramers containing the 1MH chiral end group, spacer group $n=11>n=6$, again except when a:b=1:1.

3.3.3. *The effect of the chiral end group structure on SmC* thermal stability and glass/crystalline transition temperatures*

The SmC* ranges for all the cyclic siloxane tetramers was always in the order: 2MB > 2MH. The consequence of the effects of the chiral end group on the thermal properties of the compounds was that compounds giving the widest SmC* phases came mainly from the MB series, whereas compounds giving room temperature or near room temperature SmC* phases came from the MH series. For example compound **C4**, **3d** exhibited a SmC* range of 125.5°C, **C4**, **3g** of 113.9°C, **C4**, **3b** 112.8°C and **C4**, **3k** 107.7°C.

However, the most dramatic effect of the chiral end group on the liquid crystalline behaviour of the tetramers can be found in comparing tetramers **C4**, **3f** and **C4**, **3g** from the 2MB series with tetramers **C4**, **3n** and **C4**, **3o** from the 1MH series. If we compare the liquid crystalline behaviour of **C4**, **3n** and **C4**, **3f** ($n=11$, $a=1$, $b=2$), then by changing the chiral end group from 1-methylheptyl (1MH) to 2-methylbutyl (2MB) we have changed the phase exhibited by these tetramers from SmC* to N*. In comparing tetramers **C4**, **3o** and **C4**, **3g** ($n=9$, $a=2$, $b=1$), a similar change in the chiral end group has changed the phase exhibited by these tetramers from SmA to SmC*.

4. Conclusions

All the cyclic siloxane tetramers, except tetramers **C4**, **3f** (N* only) and **C4**, **3o** (SmA only), exhibited a SmC* phase, with 6 out of the 16 cyclic siloxane tetramers also exhibiting a N* phase. Of the 16 cyclic siloxane tetramers synthesized, only one tetramer, **C4**, **3m**, gave a glass transition temperature, the remaining 15 exhibited a crystalline transition. For the two series of cyclic siloxane tetramers studied it is possible to identify trends in their liquid crystalline behaviour.

(1) Increasing the length of the spacer group or the number of phenyl rings in the mesogenic side

chain generally increased both the crystalline and mesophase transition temperatures.

(2) The effect of the arrangement of the phenyl rings on the thermal stability of the SmC* phase was variable, and depended on both the length of the spacer group and the structure of the chiral end group.

(3) The effect of changing the chiral end group from 2-methylbutyl to 1-methylheptyl generally resulted in an overall reduction in (*a*) the thermal stability of the mesophases, (*b*) the glass or crystalline transition temperatures and (*c*) the SmC* ranges exhibited by the cyclic siloxane tetramers.

(4) A very unusual result was observed for the four three-ring tetramers containing a $-(CH_2)_9-$ spacer group. Changing the chiral end group from 2-methylbutyl to 1-methylheptyl always led to a reduction in the thermal stability of the phase and in the case of tetramers **C4**, **3g** and **C4**, **3o**, we also observed a decrease in the ordering of the phase, i.e. from a SmC* phase to a SmA phase. However, we observed the formation of a more ordered phase in going from **C4**, **3f** (2MB analogue) to **C4**, **3n** (1MH analogue), i.e. from a chiral nematic phase to a SmC* phase.

(5) In general, the widest SmC* ranges came from tetramers in the 2MB series, but room/near room temperature SmC* phases were exhibited by tetramers from the 1MH series.

(6) For a given chiral end group the effect of the length of the spacer group on, (*a*) SmC* thermal stability and (*b*) glass transition/crystalline transition temperatures depended greatly on the arrangement of the phenyl rings in the mesogenic side chain. However, in general, increasing the length of the spacer group gave higher SmC* thermal stabilities and glass/crystalline transition temperatures.

This work has produced a variety of cyclic siloxane tetramers exhibiting wide range room temperature SmC* ferroelectric phases for use in ferroelectric display devices. A selection of these is: **C4**, **3m** −22.1 SmC* 42.9 I; **C4**, **3a** Cr 7.5 SmC* 31.0 I; **C4**, **3j** Cr 31.7 SmC* 114.9 I; **C4**, **3k** Cr 32.9 SmC* 140.6 I (°C).

We would like to thank the following for their contribution to this work. DRA, Malvern, for financial support to Mr T. E. Mann and Mrs J. Haley. The authors would also like to thank Prof. J. W. Goodby and Dr A. W. Hall, University of Hull, for useful discussions on phase identification. This work is presented with the kind permission of the Director of HMSO.

References

[1] Percec, V., and Hann, B., 1989, *J. polym. Sci. polym. Chem.*, **27,** 2367.

[2] Walba, D. M., Zummach, D. A., Wand, M. D., Thumes, W. N., Moray, K. M., and Arnett, K. E., 1993, *Proc. SPIE*, **1911,** 21.

[3] Poths, H., Wischerhoff, E., Zentel, R., Schonfeld, A., Henn, G., and Kremer, F., 1995, *Liq. Cryst.*, **18,** 811.

[4] Grueneberg, K., Naciri, J., Wolff, D., and Shashidhar, R., 1996, *Proc. SPIE*, **2651,** 186.

[5] Simmonds, D. J., 1992, *Liquid Crystal Polymers; from Structure to Applications*, edited by A. A. Collyer (London: Elsevier Applied Science), p. 349.

[6] Eberle, H.-J., Miller, A., and Kreuzer, F.-H., 1989, *Liq. Cryst.*, **5,** 907.

[7] Ortler, R., Brauchle, C., Miller, A., and Riepl, G., 1989, *Makromol. Chem. rapid Commun.*, **10,** 185.

[8] Kreuzer, F.-H., Dinrejewski, D., Haas, W., Haberle, N., Riepl, G., and Spes, P., 1991, *Mol. Cryst. liq. Cryst.*, **199,** 345.

[9] Bunning, T. J., Klej, L. H. E., Samukski, E. T., Drane, R. L., and Linville, R. J., 1991, *Liq. Cryst.*, **10,** 445.

[10] Mann, T. E., Haley, J., and Lacey, D., 1999, *J. mater. Chem.*, **9,** 353.

[11] Mann, T. E., and Lacey, D., 2000, *Liq. Cryst.*, **2,** 299.